Cite this as: Journal of Molecular Structure 1219 (2020) 129060

Asymmetric Schiff base ligand enables synthesis of fluorescent and near-IR emitting lanthanide compounds

Samira Gholizadeh Dogaheh [a], Janet Soleimannejad[a,*], E. Carolina Sanudo [b,c]

[a] School of Chemistry, College of Science, University of Tehran, P.O. Box 14155-6455, Tehran, Iran
[b] Secció de Química Inorgànica, Departament de Química Inorgànica i Orgànica, C/MArtí i Franqués 1-11, Universitat de Barcelona, 08028, Barcelona, Spain
[c] Institut de Nanociència i Nanotecnologia, IN2UB, Universitat de Barcelona, 08028, Barcelona, Spain

a r t i c l e i n f o

Article history:
Received 11 June 2020
Revised 7 August 2020
Accepted 10 August 2020
Available online 11 August 2020

Keywords:
Asymmetric Schiff base ligands
Fluorescence
Lanthanide(iii) complex
Chef effect
near-IR

a b s t r a c t

In this paper, the $HYDRAVH_2$ ligand as an asymmetric fluorescence Schiff base ligand was used to produce a series of new lanthanide complexes (HYDRAV-Ln(III), Ln: Yb, Er, Gd and Dy). The structures of the Schiff base complexes are characterized using Fourier transform infrared spectroscopy (FT-IR), MALDI-TOF mass spectrometry, CHN elemental analysis, Ultraviolet-Visible (UV–Vis), fluorescence, near-infrared (NIR) and thermogravimetric analysis (TGA). The photoluminescence properties show that the energy transfer from $HYDRAVH_2$ to Ln(III) ions is effective and the energy levels of $HYDRAVH_2$ and Ln(III) ions match well, therefore the Ln-compounds exhibit emission in the visible region. The result of the photophysical properties of HYDRAV-Ln(III) also indicates that strong and characteristic Near-IR luminescence for HYDRAV-Yb and HYDRAV-Er are observed, which are attributed to the antenna effect of the $HYDRAVH_2$ ligands that harvest the light and transfer it to the metal centers. Based on the above results, the ligand and its complexes (HYDRAV-Ln(III)) have remarkable optical features that could be of great utility in optoelectronic devices.

1. Introduction

Schiff bases are very popular ligand that include an azomethine (-CH =N-) or an imine (-C = N-) group that generally formed by the condensation of active carbonyl groups and amino compounds in which the nitrogen atom is bonded to an aryl or alkyl group [1-3]. Schiff bases ligands as polydentate ligands form a unique class of organic compounds due to their exclusive properties such as stability in different conditions, the multiplicity of donor sites, synthesis flexibility and formation of a wide range of complexes with various coordination geometries, which can play an essential role in the development of coordination chemistry. A broad spectrum of applications of Schiff bases ligands tagged them as versatile multifunctional materials [4-7]. They are classified as symmetric and asymmetric ligand based on the contracture. Symmetrical Schiff bases are thoroughly studied but asymmetrical ligands are much less studied, because of the difficulty associated with their synthesis [8]. The achievement of the Schiff-base ligands derived from *o*-vanillin (2-Hydroxy-3-methoxybenzaldehyde) brought attention towards this molecule as an interesting ligand by itself. *O*-vanillin is the main phytochemical existing in vanilla, the agent in food and cosmetic products, and its metal complexes showed considerable bioactivity [9]. The methoxy group in *o*-vanillin plays an important role in the coordination abilities of these molecules. *O*-vanillin derived ligands have been utilized to generate multi-metallic complexes with a rich structural variety and also chemical and physical properties [10].

Lanthanide(III) ions are the best ions with the largest size that are able to form stable complexes with high coordination numbers [11]. In between, lanthanide (III) complexes containing Schiff base provide a highly organized class of compounds with interesting properties such as antifungal [12], antibacterial [13], anticancer [14], catalytic [15], electroluminescence and fluorescence, sensing [16-18] biological activities [19], and unique magnetic properties [20].

Since the f-f transitions in the Ln(III) ions are parity forbidden, absorption coefficient in Ln(III)-compounds is very low, thus the photophysical properties of Ln(III) ions are very dependent on their ligands which can act as antennas or sensitizers and even protect the metal center from quenching effect of solvent molecules [21,22]. The $\pi\pi$-conjugated ligands are usually used as antennas, because of their greater efficiency in absorbing incident light with consequent energy transfer to lanthanide ions' excited states [23]. Therefore, stronger photoluminescence emission with color purity of the emitted light occurs for luminescent lanthanide compounds

* Corresponding author.
E-mail address: janet_soleimannejad@khayam.ut.ac.ir (J. Soleimannejad).

which can be used for applications such as imaging agents, lighting systems and lasers [24-26] where the electronic structure of lanthanide ions such as Er^{3+}, Ho^{3+} and Yb^{3+} act as the active material for optical amplification of near-IR (NIR) signals [27-28]. Additionally, in the design of lanthanide complexes for achieving the effective energy transfer from the chromophores to the Ln(III) ions, it is necessary to avoid non-radiative processes (luminescent quenching effect) in close proximity to the metal center such as the presence of -OH, -CH and -NH bonds oscillators [29].

Following our previous studies on asymmetric Schiff base ligands [30-32], here we report the synthesis and characterization of a series of new fluorescent lanthanide(III) complexes (Ln: Yb, Er, Gd and Dy) based on 1-[(2–hydroxy-3–methoxy–benzylidene)-hydrazonomethyl]-naphthalen-2-ol ($HYDRAVH_2$) ligand. Inclusion of $HYDRAVH_2$ in the Ln(III)-complexes (Ln: Yb, Er, Gd and Dy) resulted in the fluorescence enhancement due to the chelation enhanced fluorescence effect (CHEF) with the fluorescent naphthyl group in the $HYDRAVH_2$ ligand being the main contributor to the observed emission spectra. The $HYDRAVH_2$ ligand support the formation of unique assemblies for ytterbium and erbium, that display particularly enhanced emission properties in NIR.

2. Experimental

2.1. Materials

All chemicals were purchased from commercial sources and used as received. $HYDRAVH_2$ (1-[(2–hydroxy-3–methoxy–benzylidene)-hydrazonomethyl]-naphthalen-2-ol) was synthesized according to our literature methods [30].

2.2. Instrumentation

The infra-red spectra were carried out as pressed KBr discs, using Bruker Enquinox 55 spectrophotometer in the region of 400–4000 cm^{-1}. Melting points were measured on an Electrothermal 9100 apparatus. Thermogravimetric analyses (TGA) were carried out under air atmosphere on a SDT Q600 V20.9 Build 20 instrument at the heating rate of 20 °C min^{-1}. Fluorescence and near-IR measurements were taken using a NanoLogTM-Horiba JobinYvon iHR320 spectrophotometer and 9,10-diphenylanthracene was used as a standard to calculate quantum yields. UV–Vis spectra were acquired using a Cary 100 Scan from Varian in the range of 200–800 nm. Elemental analyses for C, H, and N were obtained on a LECO Truspec instrument. Positive and negative ion ESI analyses and MALDI-TOF were collected at the Unitat d'Espectrometria de Masses (CCiTUB) of the University of Barcelona.

2.3. Synthesis of ligand ($HYDRAVH_2$)

The $HYDRAVH_2$ ligand synthesized in the two steps [30]. *Step* 1) A solution of 2–hydroxy-1-naphtlaldehyde (1.74 g, 10.2 mmol) in methanol was added dropwise to hydrazine hydrate (98%) (2.5 ml, 50.6 mmol) at room temperature for an hour. A yellow precipitate formed and was collected by filtration and washed with ether. Yield 67%; m.p. 150–151 °C.

Step 2) 1-(hydrazineylidenemethyl)-naphthalen-2-ol (0.558 g, 2.99 mmol) is dissolved in 20 mL methanol. To this, a solution of 0.456 g (2.99 mmol) of 2–hydroxy-3-methoxybenzaldehyde in 20 mL methanol was added. The resulting solution was refluxed for 3 h. The obtained yellow precipitate was filtered off and washed three times with methanol and then dried with anhydrous diethyl ether. Yield: 70%; m.p. 222–223 °C. Selected IR data (KBr, cm^{-1}): 3425 (w), 2966 (w), 2846 (w), 1616 (s), 1545 (w), 1465 (s), 1316 (m), 1256 (s), 1185 (m), 1085 (w), 971 (w), 781 (m), 737 (s). ^1H NMR (DMSO–d_6, 300 MHz, ppm): δ 9.88(s,1H), 9.08(s,1H), 8.64 (d, 1H, J = 8.61 Hz), 8.04 (d, 1H, J = 9 Hz), 7.92 (d, 1H, J = 7.75 Hz),7.63 (t, 1H, J = 8.25 Hz), 7.45 (t, 1H, J = 7.17 Hz), 7.33 (d, 1H, J = 7.9 Hz), 7.27 (d, 1H, J = 8.98 Hz), 7.16 (d, 1H, J = 8.00 Hz), 6.96 (t, 1H, J = 7.91 Hz), 3.86(s, 3H). λ_{max} (nm) ($\varepsilon(M^{-1}cm^{-1})$): 229 (66,637.8), 276 (22,804.8), 332 (22,510.3) and 387 (28,139.3) in CH_3CN. ESI-MS: MW ($C_{19}H_{16}N_2O_3$) = 320.12, *m/z* (M + 1H±) = 321.12. $C_{19}H_{16}N_2O_3$: N, 8.79; C, 70.44; H, 5.32. Experimental: N: 8.74; C 71.24; H: 5.03%.

2.4. Synthesis of Ln-complexes (Ln: Yb, Er, DY and GD)

A solution of $Ln(NO_3)_3{\cdot}xH_2O$ (0.465 mmol) in CH_3CN (5 ml) was added to a solution of ligand (0.15 g, 0.468 mmol) and Et_3N (195 µL) in CH_3CN (15 ml) and the mixture was heated under reflux for 4 h. Afterwards, the obtained precipitate was filtered off and washed three times with hot CH_3CN and dried with anhydrous diethyl ether.

2.4.1. HYDRAV-Yb

Yield: 67%. m.p. > 400 °C. Selected IR data (KBr, cm^{-1}); 3424(s), 3056(w), 2926(w), 2850(w), 1607(s), 1536(m), 1464(s), 1385(m), 1313(w), 1242(w), 1221(w), 1221(w), 1186(w), 830(w), 742(m). λ_{max} (nm) ($\varepsilon(M^{-1}cm^{-1})$): 242 (96,315), 273 (34,998), 326 (13,120) and 418 (23,647) in CH_3CN. Elemental anal. calc. for $[(C_{19}H_{14}N_2O_3)_4Yb_3][Yb(NO_3)_4(H_2O)]{\cdot}(H_2O)_4{\cdot}(CH_3CN)_5$: N 9.49; C 41.17; H 3.25. Found: N 9.13; C 40.68; H 4.00.

2.4.2. HYDRAV-Er

Yield: 60%. m.p.> 400 °C. Selected IR data (KBr, cm^{-1}); 3425(s),3056(w), 2931(w), 2847(w), 1607(s), 1535(m), 1463(s), 1385(m), 1311(w), 1221(w), 1186(w), 858(w), 742(m). λ_{max} (nm) ($\varepsilon(M^{-1}cm^{-1})$): 245 (73,723), 313 (7204), 349 (4359) and 429 (17,146) in CH_3CN. Elemental anal. calc. for $[(C_{19}H_{14}N_2O_3)_4Er_3][Er(NO_3)_4(H_2O)]{\cdot}(H_2O){\cdot}(CH_3CN)$: N 7.79; C 42.33; H 2.76%. Found: N 8.03; C 41.31; H 2.80%.

2.4.3. HYDRAV-Dy

Yield: 71%. m.p.> 400 °C. Selected IR data (KBr, cm^{-1}); 3427(s), 3055(w), 2927(w), 2850(w), 1605(s), 1534(m), 1461(s), 1385(m), 1307(w), 1220(w), 1180(w), 828(w), 742(m). λ_{max} (nm) ($\varepsilon(M^{-1}cm^{-1})$): 241 (78,111), 273 (31,374.5), 324 (13,982) and 411 (20,447) in CH_3CN. Elemental anal. calc. for $[(C_{19}H_{14}N_2O_3)_4Dy_3][Dy(NO_3)_4(H_2O)]{\cdot}(H_2O)_2{\cdot}(CH_3CN)$: N 7.91, C 40.98, H 2.76%. Found: N 8.03; C 41.33; H: 2.89%.

2.4.4. HYDRAV-Gd

Yield: 65%. m.p. > 400 °C. Selected IR data (KBr, cm^{-1}); 3424(s), 3054(w), 2938(w), 2842(w), 1605(s), 1534(m), 1460(s), 1387(m), 1305(w), 1185(w), 1086(w), 971(w), 829(w), 741(m). λ_{max} (nm) ($\varepsilon(M^{-1}cm^{-1})$): 232 (66,088), 276 (26,977), 329 (15,051) and 400 (18,422) in CH_3CN. Elemental anal. calc. for $[(C_{19}H_{14}N_2O_3)_4Gd_3][Gd(NO_3)_4(H_2O)]{\cdot}(H_2O)_2{\cdot}(CH_3CN)_2$: N 8.58; C42.02; H3.00. Found: N 7.85; C 41.80; H 2.70.

3. Results and discussion

3.1. Synthesis and preliminary characterization

Following our research carried on the design and synthesis of asymmetric Schiff base ligands and their complexes [30-32], we now use fluorescent ligand $HYDRAVH_2$ to pre- pare optically active lanthanide (III) complexes (Ln: Yb, Er, Dy and Gd). $HYDRAVH_2$ was prepared through the reac- tion of 1-(hydrazonomethyl)naphthalene-2-ol with 2–hydroxy-3-methoxybenzaldehyde in two steps and was characterized by FT-IR, EA, Proton nuclear magnetic resonance (^1H NMR), UV–Vis, Elec-

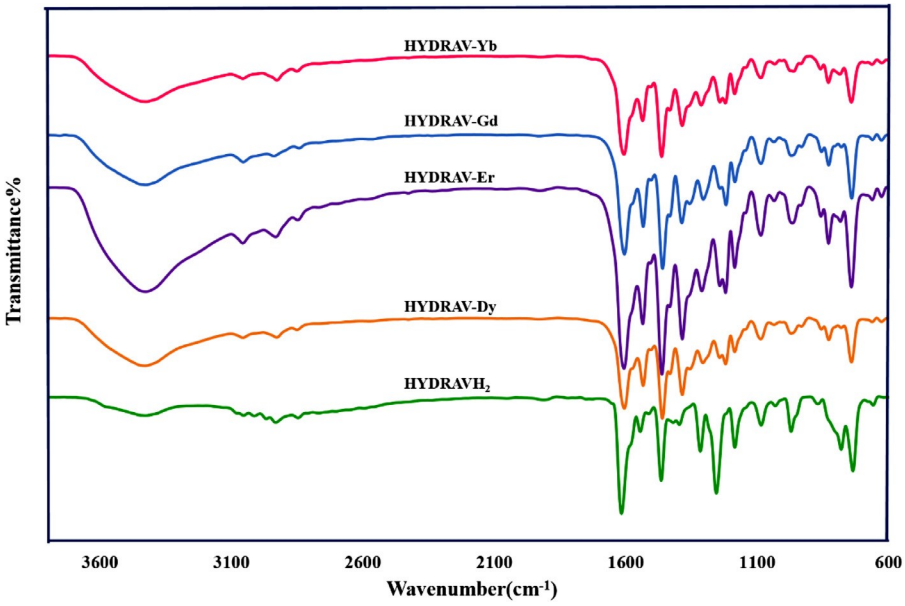

Fig 1. FT-IR spectra of the $HYDRAVH_2$ ligand and HYDRAV-Ln(III) complexes.

trospray ionization mass spectrometry (ESI mass) and single crystal X-ray diffraction (Scheme 1). $HYDRAVH_2$ can be used without further purification. The ligand is expected to be pentadentate and the possible coordination sites are phenol-oxygen (two), hydrazine-nitrogen (two) and methoxy group (one) which make this ligand a good candidate for synthesis of lanthanide coordina- tion compounds. Treatment of the ligand with $Ln(NO_3)_3.xH_2O$ (Ln: Yb, Er, Dy and Gd) in acetonitrile afforded HYDRAV-Ln(III) com- plexes. In all cases, triethylamine was used to deprotonate the two OH groups of the ligand and the product was precipitated. Differ- ent attempts to obtain single crystals, directly from the reaction or through recrystallization of the precipitate, were not successful and we only managed to get very poor quality crystals from the HYDRAV-Er compound. Therefore, the obtained crystal structure of the HYDRAV-Er compound was not good enough to be reported, but it provides an insight into the formula of the metal compound $[(HYDRAV)_4Er_3].Er(NO_3)_4.H_2O$, and of course mode of chelation of the ligand (fig. S1).

HYDRAV-Ln(III) compounds (Ln: Yb, Er, Dy and Gd) were carefully characterized by FT-IR, MALDI-TOF mass spectrometry, EA, UV–Vis and thermogravimetric analysis (TGA). The FT-IR spectrum of the HYDRAV-Ln(III) (Ln: Yb, Er, Dy and Gd) displays similar characteristics bands compared with the pure ligand (Fig. 1). A considerable red-shift of the ν(C = N) frequency is observed in the spectra of all the complexes, indicating a decrease in the stretching force constant of the C = N bond because of the coordination of the nitrogen atom of the azomethine moiety to the metal ions. This stretching band appears at *ca.* 1616 cm^{-1} for the free ligand, and in the region of 1605–1607 cm^{-1} in the spectra of all the HYDRAV-Ln(III) (Ln: Yb, Er, Dy and Gd) compounds. The sharp band at 1256 cm^{-1} corresponding to C–O in free ligand disappears in HYDRAV-Ln(III) (Ln: Yb, Er, Dy and Gd) which indicates that the ligand has coordinated to Ln^{3+} ions. The HYDRAV-Ln(III) complexes show a broad band in the 3680–3150 cm^{-1} range due to ν(OH) vibration and lattice water [33].

The infrared spectra of lanthanide complexes contain information regarding the bonding mode of NO_3^- groups. A nitrate ion can be coordinated to metal ions as monodentate, bidentate (symmetric and asymmetric chelating) and bridging bidentate ligand in various compounds [34]. Even thought, characterization of these compounds by vibrational spectroscopy is very difficult, but this technique is still useful in distinguishing between monodentate and bidentate ligands.

The bidentate NO_3^- ligand exhibits three NO stretching bands (ν(N = O), $\nu_a(NO_2)$ and $\nu_s(NO_2)$) and the separation of the two highest frequency bands of the bidentate is larger than monodentate. This rule does not apply if the complexes are significantly different [35]. However, the intensities of bands were shown to decrease in the order monodentate to bidentate [36]. The NO stretching frequencies and the magnitude of this splitting, $\Delta\nu = \nu1-\nu5$, for a number of lanthanide complexes contain bidentate nitrate groups are listed and amounts of the separation are between 116 and 159 cm^{-1} as seen in Table. S1 [37]. In our cases, the bands at *ca.* 1535 cm^{-1} and 1386 cm^{-1} are related to ν(N = O) ($\nu1$) and $\nu_{as}(NO_2)$ ($\nu5$) of the coordinated nitrate ions, respectively. The magnitude of this separation is about 149 cm^{-1} for our Ln-complexes and it suggests that the nitrate anions are coordinated to the metal ions in a bidentate fashion in all HYDRAV-Ln(III) complexes (Ln: Yb, Er, Gd and Dy).

In order to determine the molecular formula of the HYDRAV-Ln(III) compounds, MALDI-TOF mass analyses were carried out in positive modes. Fig. S2 (see supplementary data) illustrates the mass fragmentation patterns of HYDRAV-Ln(III) compounds. For all compounds, the spectrogram showed the moiety corresponding to the isotopic distribution of the $[Ln_3(HYDRAV)_4]^+$ for Ln: Yb(III), Er(III), Dy(III), Gd(III), and other fragmentation peaks of $[Gd_3(HYDRAV)_4(H_2O)]^{2+}$ (m/z:1762), thus confirming the proposed formulae and present strong witness for the formation of the HYDRAV-Ln(III) complexes.

In order to confirm the thermal stability and composition of HYDRAV-Ln(III) complexes, TGA was performed in a range of temperatures between 23 and 606 °C at a heating rate of 20 °C min^{-1} under air flow. The TGA plots are shown in Fig. 2 and the corresponding TGA data are listed in Table 1. The thermal decomposition processes of HYDRAV-Ln(III) complexes are mainly occurred in two steps: i) removal of lattice solvent molecules, ii) decomposition of the Ln(III)-complexes and ligand loss.

TGA curve for HYDRAV-Gd show the first weight loss in approximately 5.68% (calcd.5.95%) before 200 °C which is associated with the removal of the lattice solvent molecules *i.e.* water and acetonitrile. The second weight loss of 61.17% (calcd. 62.22%) occurs in the range of 200–605 °C and it is related to the de-

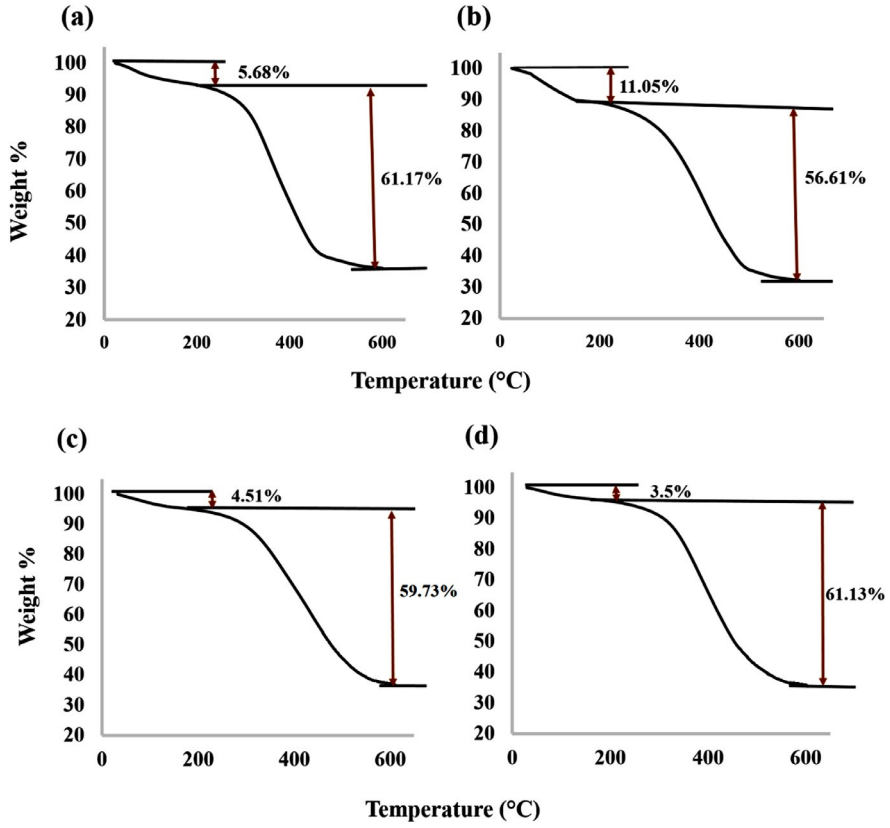

Fig. 2. TGA curves of **(a)** HYDRAV-Gd **(b)** HYDRAV-Yb, **(c)** HYDRAV-Dy and **(d)** HYDRAV-Er.

Table 1
The TGA data for HYDRAV-Ln(III).

Complexes	Loss of weigh (%) found (calculated)		
	Solvent molecules	Ligands	Residue
HYDRAV-Gd	5.68 (5.94)	61.17 (62.25)	33.16 (31.81)
HYDRAV-Yb	11.05 (11.75)	56.61 (56.71)	32.34 (31.53)
HYDRAV-Dy	4.51 (4.18)	59.73 (62.71)	35.76 (33.11)
HYDRAV-Er	3.50 (3.41)	61.13 (62.99)	35.37 (33.60)

composition of the Ln(III)-complexes and ligand loss. The total weight loss is around 66.84% (calcd. 68.17%) giving ultimately solid Gd_2O_3. Elemental analysis was performed to study the chemical composition of the HYDRAV-Gd compound and the results are in agreement with the TGA results. Therefore, the empirical formula of $[(HYDRAV)_4Gd_3][Gd(NO_3)_4(H_2O)]\cdot(H_2O)_2\cdot(CH_3CN)_2$ is considered for this compound.

As depicted in Fig. 2, the TGA curve for HYDRAV-Yb has a first step between 50 °C and 195 °C with the weight loss of 11.05%, which is related to the removal of five water and five acetonitriles molecules (the theoretical value is 11.75%). The second weight loss of 56.61% in the range of 200–606 °C is 56.61% (calcd. 56.71%) which is attributed to the detachment of the organic ligand. The total weight loss is about 67.66% emanate from the formation of Yb_2O_3 (calcd. 68.48%). According to the TGA results as well as the element analysis results, the empirical formula for HYDRAV-Yb is worked out as $[(HYDRAV)_4Yb_3][Yb(NO_3)_4(H_2O)]\cdot(H_2O)_4\cdot(CH_3CN)_5$.

The thermal stability of HYDRAV-Dy was also examined *via* TGA in the range of 23–605 °C. The results show that HYDRAV-Dy is stable up to 200 °C and decomposition takes place between 200 and 600 °C. The total weight loss is around 64.24% resulting in the formation of Dy_2O_3 (calculated 66.86%). Combining the EA results and TGA analysis, the empirical formula of the HYDRAV-Dy could be proposed as $[(HYDRAV)_4Dy_3][Dy(NO_3)_4(H_2O)]\cdot(H_2O)_2\cdot(CH_3CN)$.

For HYDRAV-Er, the results show that the compound is stable up to 200 °C and its decomposition occurs in two steps between 200 and 600 °C, which are close to the theoretical value for lattice solvent molecules (two water and one acetonitrile molecules) and burnout of the organic molecules, respectively. According to the above TGA results, as well as the element analysis results, the HYDRAV-Er formula is $[(HYDRAV)_4Er_3][Er(NO_3)_4(H_2O)]\cdot(H_2O)\cdot(CH_3CN)$. The total weight loss is around 64.63% originating from the formation of Er_2O_3 where the expected theoretical value is 66.4%.

3.2. *UV–Vis and fluorescent properties*

The photophysical properties of ligand and HYDRAV-Ln(III) (Ln: Yb, Er, Dy and Gd) complexes were recorded in dilute MeCN solution (10^{-5} M) at room temperature. The electronic spectra of HYDRAV-Ln(III) are shown in Fig. 3 and their data are listed in Table 2. The ligand absorption spectrum consists of four bands. The UV–Vis spectrum of the free ligand showed the typical absorption bands at 229 and 276 nm attributed to the $\pi - \pi^*$ transition of the aromatic rings and azomethine chromophores. While the bands at 332 nm and 387 nm were assigned to $n-\pi^*$, the forbidden transition bands of azomethine and phenol groups. Coordination of the lanthanide ions to the imine, methoxide and phenoxide groups of ligands and the deprotonation of the OH groups with change at the corresponding molecular structures are clearly observed in the UV–Vis spectra of HYDRAV-Ln(III) with a red-shift in respect to the free ligands.

The emission spectra of ligand and its complexes were collected at room temperature in acetonitrile solutions (10^{-5} M) and are shown in Fig. 3. Upon irradiation at 330 nm a strong emission

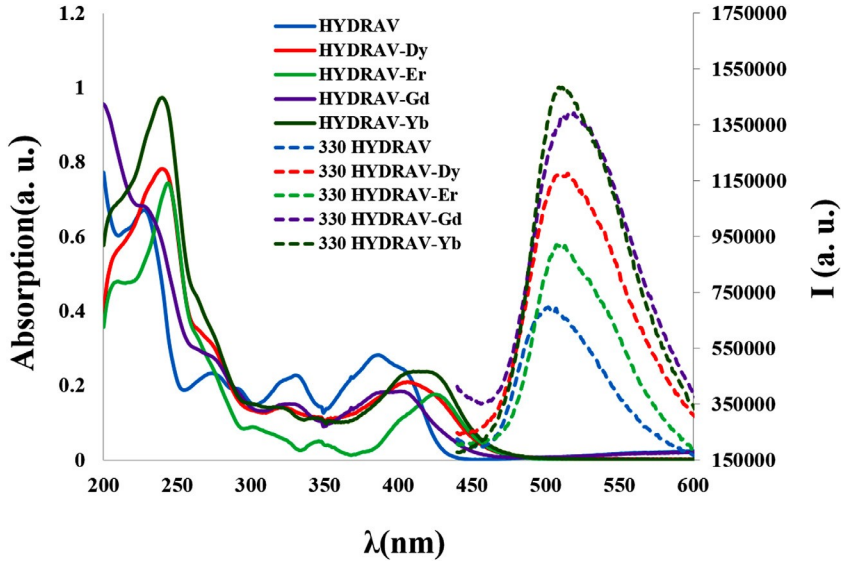

Fig 3. Electronic and emission spectra of 10^{-5} M CH_3CN solutions of $HYDRAVH_2$ and HYDRAV–Ln complexes (Ln: Dy, Er, Gd and Yb) at room temperature. Excitation wavelength: 330 nm.

Table 2
The UV–Vis data of HYDRAV-Ln(III).

Compound	λ_{max} (nm)	ε (L $mol^{-1}cm^{-1}$)
$HYDRAVH_2$	229	66,637
	279	22,804
	332	22,510
	387	28,139
HYDRAV-Yb	242	96,315
	273	34,998
	326	13,120
	418	23,647
HYDRAV-Er	245	73,723
	313	7204
	349	4359
	429	17,146
HYDRAV-Dy	241	78,111
	273	31,374
	324	13,982
	411	20,447
HYDRAV-Gd	232	66,088
	276	26,977
	329	15,051
	400	18,422

Table 3
Fluorescence data and quantum yield for $HYDRAVH_2$ and HYDRAV-Ln(III) compounds.

Compound	λ_{ex} (nm)	λ_{em} (nm)	Assignment	Quantum yields
$HYDRAVH_2$	330	495	$\pi\rightarrow\pi^*$	0.03
HYDRAV-Yb	330	510	$\pi\rightarrow\pi^*$	0.11
HYDRAV-Er	330	512	$\pi\rightarrow\pi^*$	0.24
HYDRAV-Dy	330	512	$\pi\rightarrow\pi^*$ $^4F_{9/2}\rightarrow{}^6H_{15/2}$ $^4F_{9/2}\rightarrow{}^6H_{13/2}$	0.09
HYDRAV-Gd	330	522	$\pi\rightarrow\pi^*$	0.09

band at 494 nm is observed which can be attributed to $\pi\rightarrow\pi^*$ transition. Upon coordination of ligand to Yb(III), Er(III), Dy(III) and Gd(III), the emission spectra are broadened and enhanced. In the emission spectra of the Gd^{3+} and Yb^{3+} complexes, the fluorescence enhancement is more than the other Ln-complexes. This has been reported earlier for complexes with suitable metal ion and fluorescent ligands which is referred to as the chelation-enhanced fluorescence effect (CHEF) and leads to 'turn-on' fluorescence [38-41]. Intermolecular energy transfer between the fluorescent ligands and lanthanide ions is one of the most significant processes, which can influence the fluorescent properties. In fact, the organic ligand act as the sensitizer to enhance the lanthanide fluorescent through harvesting the light and transferring it to the lanthanide ions. These compounds are dual emitting as they can absorb light in the UV–Vis region of the spectrum and then emit in both the UV–Vis region (due to the ligand) and visible/near-IR (due to lanthanide ions). The photophysical properties of compounds with several aromatic groups are unique, as energy can be transfer from π-conjugated organic chromophores to the lanthanide centers and in this way, the low molar absorptivity of the lanthanide 4f levels will be overcome and increases the ligand-centered emission (CHEF effect).

Obviously, upon complexation between Ln(III) ions and the $HYDRAVH_2$ ligand through imine (−CH=N), the benzoic −OH and −OMe groups, an increase of the electron-withdrawing ability in the complexes would induce a fluorescence enhancement. As a result, significant betterment in the fluorescence intensity of the system at about 500 nm occurs, which is attributed to a selective CHEF effect. Noticeably, sometimes lanthanide ions' emission is extremely low, which might be explained that energy transfer between ligands and metal centers is rather difficult and such effect could be due to the poor ability of the ligand to shield the metal center from non-radiative processes [42]. The HYDRAV–Ln(III) (Ln = Yb, Er, Dy and Gd) compounds reported here have different lanthanide ions with different coordination spheres. In each structure, three lanthanide ions are connected to each other by four ligands and the 4th Ln(III) ion is coordinated to a molecule of water and four nitrate ions and it is known that this lanthanide ion does not affect the fluorescence properties.

More detailed studies of fluorescence properties revealed that in addition to the $\pi\rightarrow\pi^*$ transition, some Ln(III) transitions might occur in this region *e.g.* HYDRAV-Dy(III) show $^4F_{9/2}\rightarrow{}^6H_{15/2}$ and $^4F_{9/2}\rightarrow{}^6H_{13/2}$ transitions in the same region to that of $\pi\rightarrow\pi^*$ [43]. As the result, these peaks overlaps and the peak loses its symmetry. The details of the fluorescence characteristic and quantum yield measurements [44] of the $HYDRAVH_2$ and its Ln(III) compounds are listed in Table 3.

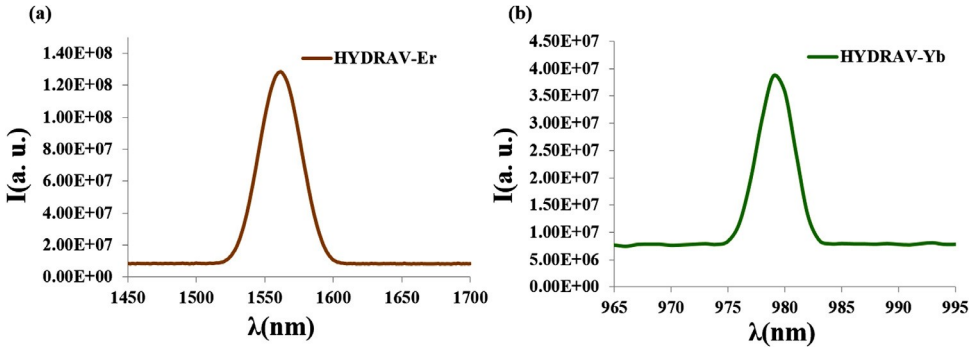

Fig 4. Solid state NIR emission of **(a)** HYDRAV-Er upon excitation at 590 nm and **(b)** HYDRAV-Yb upon excitation at 480 nm.

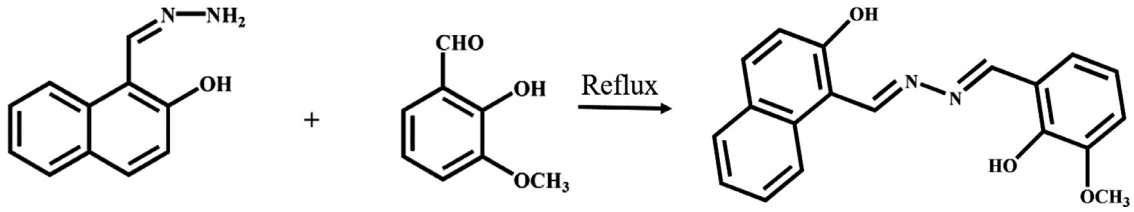

Scheme 1. Synthesis of asymmetric Schiff base ligand $HYDRAVH_2$.

NIR photoluminescence experiments on HYDRAV-Yb and HYDRAV-Er were performed at room temperature in the solid state. For HYDRAV-Er complex, irradiation at 590 nm results in a broad NIR emission peak centered at 1562 nm, which is the characteristic of Er(III) (see Fig. 4a). The free ligand does not display NIR luminescence under similar conditions. Considering that the process of emission includes three steps of the energy absorption by ligand; transferring it to lanthanide ions, and fluorescence emission by lanthanide ions, matching the triplet energy level of the ligand with the excited state energy level of the lanthanide ions is a precondition for the synthesis of a lanthanide complex having the strongest luminescent intensity [45]. Upon excitation at 480 nm, a signal at 979 nm is observed in the NIR emission spectra of HYDRAV-Yb which corresponds to the $^2F_{5/2} - ^2F_{7/2}$ electronic transition, characteristic emission band of Yb(III) (Fig. 4b). The light absorption of this band is very low in biological tissues and blood. For this reason, deep tissues and organs can be imaged and detected using a near-IR fluorescent probe containing Yb(III) ions [46]. Both HYDRAV-Er and HYDRAV-Yb show characteristic emission peaks of Er(III) and Yb(III) ions, respectively, that indicate the energy transfer from ligand to Ln(III) ions is effective, and the energy levels of ligand and Ln(III) ions are matched well.

4. Conclusions

The $HYDRAVH_2$ ligand as an asymmetric fluorescence Schiff base ligand was used to synthesis of a series of new Er(III), Yb(III), Gd(III) and Dy(III) complexes. The $HYDRAVH_2$ ligand has five possible coordination sites in its constructer and it is a proper choice for the formation of hetero- and homo-metallic Ln-complexes. The $HYDRAVH_2$ ligand is especially interesting as i) it acts as a good sensitizer that transfers the absorbed energy to the central lanthanide ions *via* antenna effect followed by the characteristic emission of the Ln(III) ions. ii) it shields the central Ln(III) ions from the inactive process such as coordination of solvent, therefore prevents quenching of their luminescence. In summary, the lanthanide complexes reported here are especially interesting due to this fact that, HYDRAV-Ln(III) (Ln: Yb(III), Er(III), Dy(III) and Gd(III)) enhanced the fluorescence intensity by the CHEF mechanism and show strong emission properties in both the UV–Vis region, due to asymmetric Schiff base ligands and in the near-IR region, due to lanthanide ions. Both HYDRAV-Yb and HYDRAV-Er show characteristic emission peaks of Yb(III) and Er(III) ions, indicating that the energy transfer from the organic ligands to lanthanide ions is effective, and the energy levels of organic ligands and lanthanide ions are matched well.

CRediT author statement

J. Soleimannejad: Supervision, Writing - review & editing.

Samira Gholizadeh Dogaheh: Conceptualization, Investigation, Formal analysis, Writing - Original Draft.

Carolina E. Sanudo: X-ray crystallography analysis, Formal analysis.

Declaration of Competing Interest

The authors declare that they have no known competing financial interests or personal relationships that could have appeared to influence the work reported in this paper.

Acknowledgements

JS and SG acknowledge support from the Iranian National Science Foundation: INSF # 97002793. ECS acknowledges financial support from the Spanish Government (Spanish Ministry of Science and Innovation, PGC2018–098630-B-I00).

Supplementary material

Supplementary material associated with this article can be found, in the online version, at doi:10.1016/j.molstruc.2020.129060.

References

[1] F.M. García-Valle, V. Tabernero, T. Cuenca, M.E.G. Mosquera, J. Cano, Intramolecular C−F activation in schiff-base alkali metal complexes, Organometallics 38 (2019) 894–904, doi:10.1021/acs.organomet.8b00868.

[2] X. Huang, R. Wang, T. Jiao, G. Zou, F. Zhan, J. Yin, L. Zhang, J. Zhou, Q. Peng, Facile preparation of hierarchical AgNP-Loaded MXene/Fe3O4/polymer nanocomposites by electrospinning with enhanced catalytic performance for wastewater treatment, ACS Omega 4 (2019) 1897–1906, doi:10.1021/acsomega.8b03615.

[3] K. Görgün, H.C. Sakarya, M. Özkütük, The synthesis, characterization, acid dissociation, and theoretical calculation of several novel benzothiazole Schiff base derivatives, J. Chem. Eng. Data 60 (2015) 594–601, doi:10.1021/je500679w.

[4] K. Mohanana, S.N. Devi, Synthesis, characterization, thermal stability, reactivity, and antimicrobial properties of some novel Lanthanide(III) complexes of 2-(N salicylideneamino)-3-carboxyethyl-4,5,6,7-tetrahydrobenzo[b]thiophene, Russian J. Coordin. Chem. 32 (2006) 600–609, doi:10.1134/S1070328406080124.

[5] J. Losada, I. del Peso, L. Beyer, Electrochemical and spectroelectrochemical properties of copper(II) Schiff-base complexes, Inorganica Chim Acta 321 (2001) 107–115, doi:10.1016/S0020-1693(01)00511-4.

[6] M. Bingol, N. Turan, Schiff base and metal (II) complexes containing thiophene-3-carboxylate: synthesis, characteriz ation and antioxidant activities, J. Mol. Struct. 1205 (2020) 127542, doi:10.1016/j.molstruc.2019.127542.

[7] T.H. Sanatkara, A. Khorshidia, E. Sohoulib, J. Janczak, Synthesis, crystal structure, and characterization of two Cu(II) and Ni(II) complexes of a tetradentate N_2O_2 Schiff base ligand and their application in fabrication of a hydrazine electrochemical sensor, Inorganica Chim. Acta 506 (2020) 119537, doi:10.1016/j.ica.2020.119537.

[8] S. Alimirzaei, M. Behzad, S. Abolmaali, Z. Abbasi, Mixed-ligand copper complexes with unsymmetrical tridentate Schiff base ligands and 2,2-bipyridine: synthesis, x-ray crystallography and antibacterial properties, J. Mol. Struct. 1200 (2020) 127148,doi:10.1016/j.molstruc.2019.127148.

[9] A. De, H. Prakash Ray, P. Jain, H. Kaur, N. Singh, Synthesis, characterization, molecular docking and DNA cleavage study of transition metal complexes of o-vanillin and glycine derived Schiff base ligand, J. Mol. Struct. 1199 (2020) 126901, doi:10.1016/j.molstruc.2019.126901.

[10] M. Andruh, The exceptionally rich coordination chemistry generated by Schiff-base ligands derived from o-vanillin, Dalton Trans. 44 (2015) 16633–16653, doi:10.1039/C5DT02661J.

[11] Q. Ain, S.K. Pandey, O.P. Pandey, S.K. Sengupta, Synthesis, spectroscopic, thermal and antimicrobial studies of neodymium(III) and samarium(III) complexes derived from tetradentate ligands containing N and S donor atoms, Spectrochim. Acta Part A: Mol. Biomol. Spectrosc. 140 (2015) 27–34, doi:10.1016/j.saa.2014.12.040.

[12] A.-N.M. Alaghaz, Y.A. Ammar, H.A. Bayoumi, S.A. Aldhlmani, molecular modeling and antimicrobial activity of new potentially N_2O_2 Azo-dye Schiff base complexes, J. Mol. Struct. 1074 (2014) 359–375, doi:10.1016/j.molstruc.2014.05.078.

[13] H. Naeimi, K. Rabiei, F. Salimi, Rapid, efficient and facile synthesis and characterization of novel Schiff bases and their complexes with transition metal ions, Dyes and Pigments 75 (2007) 294–297, doi:10.1016/j.dyepig.2006.06.001.

[14] A. Garoufis, S. Hadjikakou, N. Hadjiliadis, Palladium coordination compounds as anti-viral, anti-fungal, anti-microbial and anti-tumor agents, Coordin. Chem. Rev. 253 (2009) 1384–1397, doi:10.1016/j.ccr.2008.09.011.

[15] D. Pandiarajan, R. Ramesh, Ruthenium(II) half-sandwi ch complexes containing thioam structures and catalytic trans fer hydrogenation of ketones, J. Organomet. Chem. 723 (2013) 26–35, doi:10.1016/j.jorganchem.2012.10.003.

[16] X. Liu, C. Manzur, N. Novoa, S. Celedón, D. Carrillo, J.-R. Hamon, Multidentate unsymmetrically-substituted Schiff bases and their metal complexes: synthesis, functional materials properties, and applications to catalysis, Coordin Chem. Rev. 357 (2018) 144–172, doi:10.1016/j.ccr.2017.11.030.

[17] S. Dayan, N.K. Ozpozan, N. Özdemir, O. Dayan, Synthesis of some ruthenium(II) Schiff base complexes bearing sulfonamide fragment: new catalysts for transfer hydrogenation of ketones, J. Organomet. Chem. 770 (2014) 21–28, doi:10.1016/j.jorganchem.2014.08.002.

[18] K. Buldurun, M. Özdemir, Ruthenium (II) complexes with pyridine-based Schiff base ligands: synthesis, structural characterization and catalytic hydrogenation of ketones, J. Mol. Struct. 1202 (2020) 127266, doi:10.1016/j.molstruc.2019.127266.

[19] H. Kargar, V. Torabi, A. Akbari, R. Behjatmanesh-Ardakani, A. Sahraei, M.N. Tahir, Pd(II) and Ni(II) complexes containing an asymmetric Schiff base ligand: synthesis, x-ray crystal structure, spectroscopic investigations and computational studies, J. Mol. Struct. 1205 (2020) 127642, doi:10.1016/j.molstruc.2019.127642.

[20] S. Radhika, M. Kanthimathi, R. Parthasarathi, B.U. Nair, Europium complex of a tridentate ligand: synthesis and spectroscopic properties, Trans. Metal Chem. 32 (2007) 362–366, doi:10.1007/s11243-006-0180-4.

[21] X. Yang, R.A. Jones, W.-K. Wong, Pentanuclear tetra-decker luminescent lanthanide Schiff base complexes, Dalton Trans. (2008) 1676–1678, doi:10.1039/b801513a.

[22] C. Wang, S. Wang, L. Bo, T. Zhu, X. Yang, L. Zhang, D. Jiang, H. Chen, S. Huang, Synthesis, crystal structures and NIR luminescence properties of binuclear lanthanide Schiff Base complexes, Inorg. Chem. Commun. 85 (2017) 52–55, doi:10.1016/j.inoche.2017.06.003.

[23] L.A. Galán, A.N. Sobolev, B.W. Skelton, E. Zysman-Colman, M.I. Ogden, M. Massi, Energy transfer between Eu^{3+} and Nd^{3+} in near-infrared emitting β-Triketonate coordination polymers, Dalton Trans. 47 (2018) 12345–12352, doi:10.1039/C8DT02499E.

[24] J.-C.G. Bünzli, C. Piguet, Structure, magnetic and luminescence properties of the lanthanide complexes $Ln_2(Salphen)_3\ H_2O$ (Ln = Pr, Nd, Sm, Eu, Gd, Tb, Dy; H_2Salphen = N,N0-bis(salicylidene)-1,2 phenylenediamine, Chem. Soc. Rev. 34 (2005) 1048–1077, doi:10.1016/j.ica.2014.01.034.

[25] K. Binnemans, Taking advantage of luminescent lanthanideions, Chem. Rev. 109 (2009) 4283–4374, doi:10.1039/B406082M.

[26] A. D'Aléo, F. Pointillart, L. Ouahab, C. Andraud, O. Maury, Charge transfer excited states sensitization of lanthanide emitting from the visible to the near-infra-red, Coordin. Chem. Rev. 256 (2012) 1604–1620, doi:10.1016/j.ccr.2012.03.023.

[27] L. Slooff, A. Van Blaaderen, A. Polman, G. Hebbink, S. Klink, F. Van Veggel, D. Reinhoudt, J. Hofstraat, Rare-earth doped polymers for planar optical amplifiers, J. Appl. Phys. 91 (2002) 3955–3980, doi:10.1063/1.1454190.

[28] Z. Ye, M. Tan, G. Wang, J. Yuan, Preparation, characterization, and time-resolved fluorometric application of silica-coated terbium(III) fluorescent nanoparticles, Anal. Chem. 76 (2004) 513–518, doi:10.1021/ac030177m.

[29] W. Feng, Y. Zhang, X. L€u, Y. Hui, G. Shi, D. Zou, J. Song, D. Fan, W.-K. Wong, R.A. Jones, Near-infrared (NIR) luminescent homoleptic lanthanide Salen complexes Ln4(Salen)4 (Ln: nd, Yb or Er), Cryst. Eng. Commun., 14(2012) 3456, 10.1039/C2CE06566E

[30] S.G. Dogaheh, H. Khanmohammadi, E.C. Sañudo, A new trinuclear N–N bridged Cu(II) complex with an asymmetric Schiff base ligand derived from hydrazine, Polyhedron 133 (2017) 48–53, doi:10.1016/j.poly.2017.05.010.

[31] S.G. Dogaheh, H. Khanmohammadi, E.C. Sañudo, Double-decker luminescent ytterbium and erbium SMMs with symmetric and asymmetric Schiff base ligands, N. J. Chem. 41 (2017) 10101–10111, doi:10.1039/C7NJ01842H.

[32] S.G. Dogaheh, M.J. Heras Ojea, L.R. Piquer, L. Artus Suarez, H. Khanmohammadi, G. Aromí, E.C. Sañudo, CoII and CuII Fluorescent Complexes with Acridine-Based Ligands, Eur. J. Inorg. Chem. 2016 (2016) 3314–3321, doi:10.1002/ejic.201600297.

[33] A. El-Tabl, R. Issa, M. Morsi, Synthesis and characterization of chromium(III), molybdenum(III), ruthenium(III) and osmium(III) complexes with N_2O_2–Schiff bases of 2-hydroxy-1-naphthaldimines, Trans. Metal Chem. 29 (2004) 543–549.

[34] N. Curtis, Y.M. Curtis, Some nitrato-amine nickel(II) compounds with monodentate and bidentate nitrate ions, Inorg. Chem. 4 (1965) 804–809, doi:10.1021/ic50028a007.

[35] K. Nakamoto, Infrared and Raman spectra of inorganic and coordination compounds, Handbook of Vibrational Spectroscopy, (2006), DOI: 10.1002/9780470027325.s4104

[36] A.B.P. Lever, E. Mantovani, B.S. Ramaswa, Infrared combination frequencies in coordination complexes containing nitrate groups in various coordination environments. a probe for the metal-nitrate interaction, Can. J. Chem. 49 (1971) 1957–1964, doi:10.1139/v71-315.

[37] M. Gaye, F.B. Tamboura, A.S. Sall, spectroscopic studies of some lanthanide(III) nitrate complexes synthesized from a new ligand 2,6-bis-(salicylaldehyde hydrazone)-4-chlorophenol, Bull. Chem. Soc. Ethiop. 17 (2003) 27–34, doi:10.4314/bcse.v17i1.61726.

[38] C. Varadaraju, M.S. Paulraj, G. Tamilselvan, I.M.V. Enoch, V. Srinivasadesikan, L. Shyi-Long, Evaluation of metal ion sensing behaviour of fuorescent probe along with its precursors: PET-CHEF mechanism, molecular logic gate behaviour and DFT studies, J. Incl. Phenom. Macrocycl. Chem. 95 (2019) 79–89, doi:10.1007/s10847-019-00919-5.

[39] A. Sahana, A. Banerjee, S. Lohar, B. Sarkar, S.K. Mukhopadhyay, D. Das, Rhodamine-based fluorescent probe for Al^{3+} through time dependent PET −CHEF −FRET processes and its cell staining application, Inorg. Chem. 52 (2013) 3627–3633, doi:10.1021/ic3019953.

[40] A.S. Gupta, K. Paul, V. Luxami, A new 'turn-on' PET-CHEF based fluorescent sensor for Al^{3+} and CN^-ions: applications in real samples, Anal. Methods 10 (2018) 983–990, doi:10.1039/C7AY02779F.

[41] A. Bhattacharyya, S.C. Makhal, N. Guchhait, CHEF-affected fluorogenic nanomolar detection of Al^{3+} by an anthranilic acid −naphthalene hybrid: cell imaging and crystal structure, ACS omega 3 (2018) 11838–11846, doi:10.1021/acsomega.8b01639.

[42] L. Wang, J. Tang, N. Sui, X. Yang, L. Zhang, X. Yao, Q. Zhou, H. Xiao, S. Kuang, W.W. Yu, A highly selective Schiff base fluorescent chemosensor for Lu^{3+}, Anal. Methods 9 (2017) 6254–6260, doi:10.1039/c7ay01808h.

[43] Z.A. Tahaa, A.M. Ajlouni, K.A. Al-Hassan, A.K. Hijazi, A.B. Faiq, Syntheses, characterization, biological activity and fluorescence properties of bis-(salicylaldehyde)-1,3-propylenediimine Schiff base ligand and its lanthanide complexes, Spectrochimica Acta Part A 81 (2011) 317–323, doi:10.1016/j.saa.2011.06.018.

[44] C. Würth, M. Grabolle, J. Pauli, M. Spieles, U. Resch-Genger, Relative and absolute determination of fluorescence quantum yields of transparent samples, nature protocols, 8 (2013) 1535–1550, doi:10.1038/nprot.2013.087

[45] L. Li, J. Gou, D.-F. Wu, Y.-J. Wang, Y.-Y. Duan, H.-.H. Chen, H.L. Gao, J.-.Z. Cui, Near-infrared luminescence and magnetic properties of dinuclear rare earth complexes modulated by β-diketone co-ligand, N. J. Chem. 44 (2020) 3912–3921, doi:10.1039/D0NJ00164C.

[46] H. Uh, P.D. Badger, S.J. Geib, S. Petoud, Synthesis and solid-state, solution, and luminescence properties of nearinfrared-emitting neodymium (3+) complexes formed with ligands derived from salophen, Helv. Chim. Acta 92 (2009) 2313–2329, doi:10.1002/hlca.200900162.